Psychiatry Research 325 (2023) 115256

Contents lists available at ScienceDirect

Psychiatry Research

journal homepage: www.elsevier.com/locate/psychres

Unravelling brain connectivity patterns in body dysmorphic disorder during decision-making on visual illusions: A graph theoretical approach

Anastasios E. Giannopoulos [a,*,1], Ioanna Zioga [b,c,1], Caroline Di Bernardi Luft [d], Panos Papageorgiou [e], Georgios N. Papageorgiou [f], Fotini Kapsali [g], Konstantinos Kontoangelos [c], Christos N. Capsalis [a], Charalabos Papageorgiou [h]

[a] School of Electrical & Computer Engineering, National Technical University of Athens, 9, Iroon Polytechniou Str., Zografou Athens 15773, Greece
[b] Donders Institute for Brain, Cognition and Behaviour, Radboud University, Nijmegen, the Netherlands
[c] First Department of Psychiatry, National and Kapodistrian University of Athens Medical School, Eginition Hospital, 74 Vas. Sophias Ave., Athens 11528, Greece
[d] School of Biological and Chemical Sciences, Queen Mary, University of London, London E1 4NS, United Kingdom
[e] Department of Electrical and Computer Engineering, University of Patras, Patras, Greece
[f] School of Mechanical Engineering, National Technical University of Athens, Athens, Greece
[g] Psychiatric Hospital of Attica, 374 Athinon Ave., Athens 12462, Greece
[h] University Mental Health, Neurosciences and Precision Medicine Research Institute "COSTAS STEFANIS", (UMHRI), Athens, Greece

ARTICLE INFO

Keywords:
EEG
Body dysmorphic disorder
Visual illusions
Graph theory
Decision-making
Connectivity

ABSTRACT

Body dysmorphic disorder (BDD) is characterized by an excessive preoccupation with perceived defects in physical appearance, and is associated with compulsive checking. Visual illusions are illusory or distorted subjective perceptions of visual stimuli, which are induced by specific visual cues or contexts. While previous research has investigated visual processing in BDD, the decision-making processes involved in visual illusion processing remain unknown. The current study addressed this gap by investigating the brain connectivity patterns of BDD patients during decision-making about visual illusions. Thirty-six adults - 18 BDD (9 female) and 18 healthy controls (10 female) - viewed 39 visual illusions while their EEG was recorded. For each image, participants were asked to indicate (1) whether they perceived the illusory features of the images; and (2) their degree of confidence in their response. Our results did not uncover group-level differences in susceptibility to visual illusions, supporting the idea that higher-order differences, as opposed to lower-level visual impairments, can account for the visual processing differences that have previously been reported in BDD. However, the BDD group had lower confidence ratings when they reported illusory percepts, reflecting increased feelings of doubt. At the neural level, individuals with BDD showed greater theta band connectivity while making decisions about the visual illusions, likely reflecting higher intolerance to uncertainty and thus increased performance monitoring. Finally, control participants showed increased left-to-right and front-to-back directed connectivity in the alpha band, which may suggest more efficient top-down modulation of sensory areas in control participants compared to individuals with BDD. Overall, our findings are consistent with the idea that higher-order disruptions in BDD are associated with increased performance monitoring during decision-making, which may be related to constant mental rechecking of responses.

1. Introduction

Body dysmorphic disorder (BDD) is a psychiatric illness characterized by distress and excessive preoccupation with perceived defects in physical appearance that are not at all or only slightly observable to others (American Psychiatric Association, 2013). These concerns are usually focused on facial features or body parts (e.g., nose, denture, limbs). Importantly, BDD symptoms include repetitive thoughts and compulsive behaviours, due to a preoccupation with the respective concerns. This constant preoccupation is associated with many time-consuming rituals, such as skin picking, mirror gazing, excessive grooming, and constant checking (Buhlmann et al., 2002). In addition,

* Corresponding author.
E-mail address: angianno_8@hotmail.com (A.E. Giannopoulos).
[1] These authors contributed equally to this work.

https://doi.org/10.1016/j.psychres.2023.115256
Received 13 March 2022; Received in revised form 26 April 2023; Accepted 16 May 2023
Available online 18 May 2023

BDD patients often compare the appearance of others' features to their own. Due to the ritualistic nature of these symptoms, BDD was recently classified under the obsessive-compulsive and related disorders in the DSM-5, alongside obsessive-compulsive disorder (OCD) (American Psychiatric Association, 2013). Excessively checking the perceived flaw in mirrors or other reflective surfaces in BDD might thus be associated with cognitive dysfunction of the inhibition of unwanted impulses, as in OCD (Mataix-Cols et al., 2004).

As in the case of OCD, BDD patients show different attentional patterns compared to healthy controls during processing of visual stimuli, especially faces (Toh et al., 2015). For instance, BDD patients show a reduced inversion effect compared to healthy controls, which has been attributed to greater focus on detail and reduced holistic processing (Feusner et al., 2010a). The face inversion effect, i.e. the decrement in performance for processing inverted vs. upright faces, is a prominent measure of holistic processing (Bennetts et al., 2022). Stangier et al. (2008) also found enhanced sensitivity to facial feature changes in BDD patients compared to healthy controls, indicating increased detailed visual processing in BDD. Furthermore, when presented with images of their own faces, both BDD and OCD patients, but not healthy controls, perceived distortions that did not actually exist (Yaryura-Tobias et al., 2002). In another study, Buhlmann et al. (2004) found that BDD patients had difficulty interpreting facial expressions, as they often misclassified faces as being angry when that was not the case. Following from the aforementioned findings, here we examined whether BDD patients show different susceptibility to visual illusions compared to healthy controls; and investigated their brain connectivity patterns during decision-making about illusion-inducing visual stimuli, in order to shed light onto how cognitive processing in BDD differs from unaffected individuals.

Visual illusions refer to percepts that are different in some respects (e.g., length, size, shape, or direction of elements) from the physical stimulus. They are context-induced subjective distortions of visual features (Bruno, 2005; Murray and Herrmann, 2013; Sterzer and Rees, 2008) leading to ambiguous percepts (Murray and Herrmann, 2013). In many cases, illusions are perceptually experienced even though the individual is aware of the illusory features, suggesting that perceptual and conceptual knowledge are markedly distinct (Gregory, 1997). Importantly, illusions reflect the constraints of our visual system, which supports efficient visual processing of our external environment (see Eagleman, 2001 for a review). For instance, these constraints allow us to perceive the world as stable, even though we are constantly moving our head, eyes, and body. Illusions therefore provide a powerful tool to study not only the neurobiology of vision, but also other cognitive processes related to subjective experiences of the world (Eagleman, 2001; King et al., 2017). Given the subjectivity of perceived distortions produced by the visual illusions and the visual abnormalities of BDD, here we tested whether illusory percepts that are not related to the self (e.g., own face processing) would differ between BDD and control subjects.

Previous neuroscientific studies have shown differentiated structural and functional brain patterns in BDD compared to healthy individuals (e.g., Buchanan et al., 2013; see Grace et al., 2017 for a review). Specifically, BDD patients show brain activation abnormalities when processing their own face, and specifically hypoactivation of the occipital cortex potentially associated with differentiated processing of facial features, as well as frontostriatal hyperactivation possibly related to obsessive thoughts and compulsive behaviours (Feusner et al., 2010b). Two fMRI studies in which participants performed a matching task of pictures of others' faces found that local and distant degree brain connectivity of the right orbitofrontal cortex positively correlated with BDD (Beucke et al., 2016) and OCD symptom severity (Beucke et al., 2013). Overall, OCD patients show a generalized disorganization among neural tracts, as well as specific abnormalities in the frontostriatal pathway, the corpus callosum, and the superior longitudinal fasciculus (Bora et al., 2011; Garibotto et al., 2010). Besides visual processing, previous research has demonstrated cognitive impairments in BDD patients in memory and attention (e.g., Kapsali et al., 2020; Toh et al., 2015, 2017). For example, decreased alpha power during cognitive tasks in BDD and OCD has been associated with difficulties with cognitive inhibition (Perera et al., 2019). Furthermore, an EEG study using the prepulse inhibition paradigm found reduced neural inhibition of the startle tone in BDD patients compared to healthy controls, suggesting impaired sensorimotor gating and abnormalities in attention (Giannopoulos et al., 2021).

While previous research on the neurophysiological correlates of BDD has provided substantial insight into the visual processing mechanisms behind the condition, the corresponding decision-making processes remain unknown. The present study aims to fill this crucial gap by investigating the brain connectivity patterns of BDD during decision-making on visual illusion judgements. We recorded and analyzed the EEG of BDD patients and healthy controls while they evaluated visual illusions (Giannopoulos et al., 2022). Participants had to decide whether they perceived or not the illusory features of each image. To examine confidence fluctuations throughout the task, participants also reported the degree of confidence in their judgment. Besides the BDD diagnosis performed by clinical psychiatrists, participants completed two questionnaires assessing BDD symptomatology. At the behavioural level, we examined whether BDD patients differed in relation to their perception of the images and confidence in their own judgments, while at the neural level, we analyzed brain connectivity and network characteristics using graph theoretical measures during the decision-making period. Finally, the potential relationship between BDD severity and the identified graph indices was examined.

Considering that BDD patients have biased visual processing when perceiving their own faces (e.g., Yaryura-Tobias et al., 2002) rather than deficits in general visual processing, we hypothesize that the BDD group will be equally susceptible to the illusory effects as the control group. Given the compulsive behavior that characterizes BDD patients (Nedeljkovic et al., 2009), we predict that their increased feelings of doubt will be reflected in lower confidence about their answers. It is also expected that BDD patients' confidence ratings would fluctuate more compared to healthy controls, due to their compulsive performance evaluation. At the neural level, considering the constant BDD checking habits, as well as the role of midfrontal theta band activity (4–8 Hz) in performance monitoring (Cavanagh et al., 2012), we hypothesize that BDD patients will show stronger theta band interchannel phase synchronization in frontocentral electrodes during decision-making compared to healthy controls. Since disrupted interhemispheric connectivity in BDD indicates detailed processing (Buchanan et al., 2013), we also expect that BDD patients will exhibit reduced connectivity between hemispheres during decision-making, attributed to impaired holistic processing (Stangier et al., 2008).

2. Methods

2.1. Subjects

Thirty-six adult participants were included in this study. The first group consisted of 18 BDD patients (9 females, mean ± SD age of 36.7± 8.3 years; 9 males, mean ± SD age of 27.1± 6.0 years). The second group consisted of 18 healthy controls (CTL), matched for age and sex (10 females, mean ± SD age of 28.8± 4.9 years; 8 males, mean ± SD age of 30.0± 5.7 years). The absence of significant group differences in age was confirmed by an independent-samples *t*-test ($t(34) = -1.081, p = 0.287$). Participants underwent two independent clinical interviews by two psychiatrists. BDD was diagnosed according to DSM-5 criteria. The Yale-Brown Obsessive-Compulsive Scale for BDD (YBOCS-BDD) and the Dysmorphic Concern Questionnaire (DCQ) confirmed the diagnosis. All participants had normal or corrected vision, while exclusion criteria were history of neurological or psychiatric disorders and current pregnancy.

All participants were extensively informed about the procedure and gave written consent for participation. In accordance with the Declaration of Helsinki, the study was performed in the psychophysiology laboratory of the University Mental Health, Neurosciences and Precision Medicine Research Institute 'Costas Stefanis', in collaboration with the First Department of Psychiatry, Eginition Hospital, Medical School, National and Kapodistrian University of Athens. The study was approved by the local ethics committee of the First Department of Psychiatry, Medical School, Eginition Hospital, National and Kapodistrian University of Athens (protocol code 349 and date of approval 29 September 2013).

2.2. Paradigm and procedure

The visual stimuli set comprised of 39 previously tested visual illusions assembled and tested by Papageorgiou et al. (2020) (see Fig. 1A for examples). Those comprised two-dimensional images (28 black and white, 11 colored) of 23 well-known visual illusions plus their

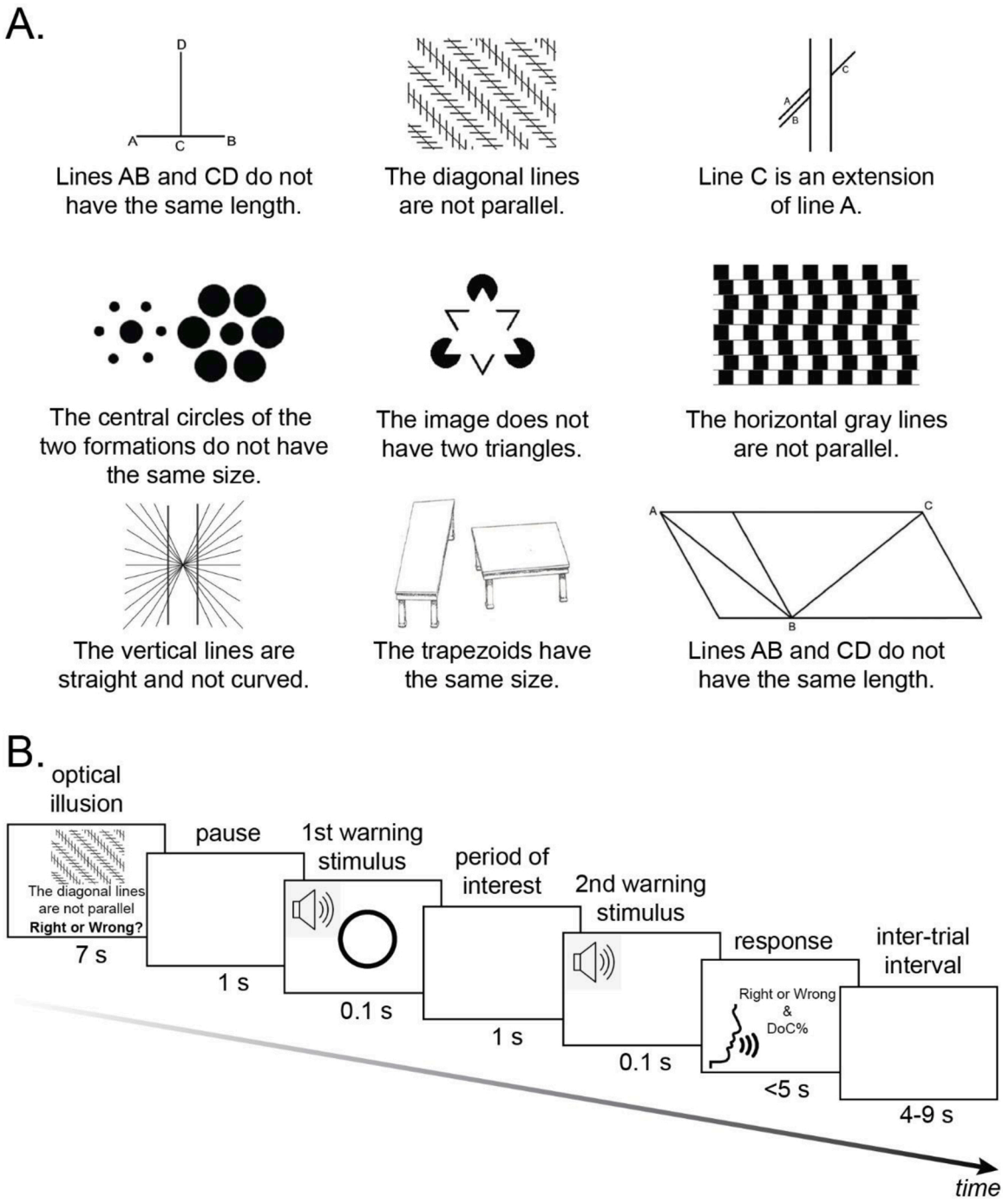

Fig. 1. A. Examples of the experimental stimuli composed by Papageorgiou et al. (2020). The illusions depicted are the following: vertical-horizontal, Zöllner, Poggendorff, Ebbinghaus, Kanizsa's triangle, café wall, Hering, Shepard tables, and Sander. The images have been obtained by the authors from Wikipedia (available under a CC BY-SA 3.0 license). **B.** Illustration of the trial structure. First, a visual illusion is presented on screen for 7 secs, together with a statement and the question Right or Wrong? Below the stimulus. A blank screen is then presented for 1 s, followed by a 0.1-s warning stimulus tone. Participants are given 1 s to think of their response. A second warning stimulus tone is then presented for 0.1 s. Afterwards, participants verbalize two responses: 1. Whether the statement is right or wrong, and 2. What is their degree of confidence for their answer. There is an inter-trial interval jittered from 4 to 9 s.

variations. The length of the images ranged from 8 to 33cm, while the height of the images ranged from 5.5 to 14.5cm. Each stimulus (i.e. visual illusion) was accompanied with a written statement referring to a feature of the respective image. Each of these statements required a 'right' or 'wrong' answer. There were 19 'right' (e.g., illusion 3 in Fig. 1A: Line C is an extension of line A.) and 20 'wrong' statements (e.g., illusion 2 in Fig. 1A: The diagonal lines are not parallel.).

Participants were seated in an electromagnetically shielded cage and they were asked to look straight and keep their eyes open throughout the session. Participants were instructed that they would be presented with 39 visual illusions together with a written statement, and would be prompted to answer two questions: 1. Whether the statement is right or wrong, and 2. What is their degree of confidence for their answer on a scale from 0 (not at all certain) to 100 (absolutely certain). Each visual illusion stimulus was presented on screen for 7 s (see Fig. 1B for the trial structure). A statement referring to the illusion was presented below the stimulus, followed by the question 'Right or Wrong?'. A blank screen was then presented for 1 s, followed by a 0.1-s warning stimulus tone (500Hz, 65dB). Then, a 1-s period was given to participants for decision-making. A second warning stimulus tone was then presented for 0.1 s prompting participants to respond. Participants' verbal responses were recorded by an experimenter seated outside the testing room. There was an inter-trial interval jittered from 4 to 9 secs.

2.3. Recordings and preprocessing

EEG recordings were obtained from 30 Ag/AgCl electrodes mounted on an elastic cap according to the International 10–20 System: Fp1, F3, P3, O1, F7, T3, T5, Afz, Fz, FCz, CP3, FC3, TP7, Fpz, FT7, Oz, FT8, Fp2, F4, C4, P4, O2, F8, T4, T6, Cz, Pz, CPz, CP4, FC4. The sampling frequency was 1000Hz. Electrode impedance was kept constantly below 5kΩ. Online reference was the average of the left and right ear lobes and the ground electrode was placed on the left mastoid. Continuous data were band-pass filtered at 0.5–40Hz to remove DC offsets and ignore the line noise. Using EEGLAB (Delorme and Makeig, 2004), we detected the channels that showed constantly abnormal activity and then replaced their data using spherical interpolation. Each channel's activity was then re-referenced to the whole-scalp common average. Eye-blinks and saccades were corrected using the Independent Component Analysis (ICA) algorithm. SASICA tool (Chaumon et al., 2015) was used to guide the selection of artifactual components, along with visual inspection of the identified artifacts. In controversial cases, we also consulted the MARA tool suggestions (Winkler et al., 2011). The SASICA guidelines were parameterized as: "Autocorrelation" (Threshold r = auto; Lag = 20ms), "Focal components" (Threshold z = auto), "Correlation with EOG" (enabled for VEOG and HEOG with threshold $r = 0.2$), "ADJUST" (Mognon et al., 2011) and "FASTER" (Nolan et al., 2010) methods (enabled for blink channels). Finally, continuous data were epoched from −0.3 to 1 s, time-locked to the first warning stimulus tone.

2.4. Psychometric questionnaires

2.4.1. Yale-Brown obsessive-compulsive scale (Y-BOCS) for BDD

We used a 12-item version of Y-BOCS assessing BDD symptom severity (Phillips et al., 1997) translated and validated in Greek (Kapsali et al., 2019). Items 1–5 assess obsessional preoccupation with the perceived defect in appearance, while items 6–10 assess compulsive behaviours. Item 11 measures the degree of insight, and item 12 measures avoidance. It is rated on a 0 (not at all) to 4 (every day) Likert scale. Scores for all items are summed up to create the total score.

2.4.2. Dysmorphic concern questionnaire (DCQ)

This is a 7-item self-report questionnaire that evaluates cognitive and behavioural symptoms of dysmorphic concern (Oosthuizen et al., 1998). Respondents rate their concern about their physical appearance on a 4-point Likert scale from 0 (not at all) to 3 (much more than most people).

2.5. Behavioural data analysis

2.5.1. Behavioural measures

The following behavioural measures were extracted from the participants' answers and their respective degree of confidence:

- *Correctness:* the percentage ratio between the correct answers and the total number of trials (39). A correct response means the participant response was aligned with the physical stimulus rather than the visual illusion.
- *Confidence:* the average self-reported confidence across trials. This measure was computed separately for the correct vs. incorrect answers.
- *Confidence variability:* the variance of the self-reported confidence across trials.

About *correctness*, note that the terms "correct", "incorrect", and "accuracy" are used throughout the manuscript by convention. Nonetheless, this measure represents how many times participants were susceptible to the visual illusions (being susceptible to an illusion does not mean a "wrong" response, rather it reflects the constraints of our visual system; see Eagleman, 2001 for a review). For instance, low correctness does not indicate poor performance, but rather a high susceptibility to illusions, which is a behavior linked to the function of our visual system.

Furthermore, to ensure that subjects did not randomly select their answers, we asked them to report their *confidence* and, in cases of random guessing, they were instructed to declare low degree of confidence (i.e. when confidence is close to zero, participants tended to respond randomly). As there is no way to know what participants perceived, confidence comprises a measure of whether participants actually saw the illusions or not. In other words, the level of confidence reveals whether responses are randomly selected or whether they are based on participants' perception.

2.5.2. Statistical analysis

Parametric statistics were used to compare the behavioural measures across groups/conditions. Independent samples *t*-tests were conducted to compare the group differences in the *correctness* and *confidence variability* measures. A 2 × 2 mixed-design ANOVA was also conducted to assess the differences in the *confidence* (between-subjects factor: CTL vs. BDD; within-subjects factor: correct vs. incorrect). The normality of data distribution and the equality of variances across groups were assessed with Shapiro-Wilk and Levene's tests, respectively. Both tests showed that the data fulfilled the basic requirements for the subsequent parametric tests (all p's>0.05). Post-hoc contrasts refer to Bonferroni-corrected p-values at 0.05, two-tailed.

2.6. Electrophysiological data analysis

2.6.1. All-to-all connectivity

Before the computation of EEG connectomes, we performed time-frequency decompositions of the EEG signals using the continuous wavelet transform (CWT) in the post-stimulus period (0 to 0.8s). Single-trial EEG signals were convolved with complex Morlet wavelets using 50 linearly-separated frequencies (from 1 to 40Hz) with cycles linearly increasing from 3 to 12. The spectral values were then grouped according to the canonical frequency bands, namely the delta (1–4 Hz), theta (4–8Hz), alpha (8–12.5Hz), beta (13–30Hz) and low gamma (30–40Hz). Subsequently, the cross-spectra density matrix was extracted for each pair of channels using the complex-valued CWT coefficients.

Based on the cross-spectrum arrays, the *undirected* functional connectivity between all pairs of channels (all-to-all connectivity) was computed by means of debiased weighted Phase Lag Index (dwPLI:

Vinck et al., 2011). As an extension of the PLI (Stam et al., 2007), dwPLI is a quantitative measure of the asymmetry in the distribution of phase differences between two signals. It is calculated from the instantaneous phases of two waveforms. Key advantages in using the dwPLI include (i) robustness against volume-conducted ('false positive') connectivity (Stam et al., 2007), (ii) insensitivity on connectivity variations caused by uncorrelated noise (Chennu et al., 2016) and (iii) correction for sample-size biases (Vinck et al., 2011). The main idea in the dwPLI calculation is (i) to ignore the zero-lag (0 or π) phases that are principally attributed to either volume-conducted or coupled activity and (ii) to weight differently the phases close to 0 or π (low influence on connectivity estimate) from the other middle phases (large influence on connectivity estimate). dwPLI values ranged from 0 (zero coupling) to 1 (max phase coupling) and were computed separately for each canonical band using the FieldTrip Toolbox (Oostenveld et al., 2011). Finally, the dwPLI value of a particular channel pair and frequency band was extracted by averaging across the respective frequency points.

Following a similar approach, we also extracted a measure of *directed* connectivity, namely the Phase Slope Index (PSI). It is a phase-based connectivity measure that indicates whether the network connectivity flows from channel A to B or vice versa (Nolte et al., 2008). Non-zero PSI values reflect the overall asymmetry of directed connectivity between two channels (PSI>0 when A is driven by B; PSI<0 when B is driven by A, PSI=0 when A and B are equally bidirectional). The PSI connectivity matrices were also extracted using FieldTrip Toolbox (Oostenveld et al., 2011) for each of the five frequency bands.

2.6.2. Thresholding of connectivity graphs

The connectivity arrays were considered as network graphs with the channels representing the nodes and the dwPLI/PSI values representing the edge weights. To retain the strong edges of the networks for the subsequent graph-theoretical analysis, we followed a thresholding procedure. Specifically, we computed a threshold connectivity value for each separate frequency band as the median plus 1 standard deviation across the absolute connectivity values of all edges. Then, the edges corresponding to below-threshold values were discarded (set to 0) from each participant's graph. We obtained a binarized graph (the edges that survived after the thresholding procedure were set to 1) and a weighted graph (the edges that survived after the thresholding procedure retained their actual values) for each participant and frequency band. Fig. 2 depicts the procedure of network graphs extraction for a particular frequency band following four steps.

To further quantify the organizational properties of the derived networks, several graph-theoretical measures were then computed from both the undirected/directed and binary/weighted graph representation, as presented below.

2.6.3. Graph theoretical measures

Given a thresholded connectivity graph, the following measures were extracted (including both global and local graph metrics):

- *Density:* the percentage of present connections to all possible connections (weights are ignored).
- *Strength:* the sum across all edge weights.
- *Degree:* the number of incoming/outcoming connections for each electrode.
- *Clustering coefficient (CC):* the fraction of triangles around a node. It reflects the extent to which the neighbors of a channel are also neighbors with each other.
- *Average Clustering coefficient (Ccavg):* the average clustering coefficients across all channels.
- *Floyd-Warshall matrix:* it contains the length of shortest path between each pair of channels according to the Floyd-Warshall algorithm. In the case of weighted matrices, the distance between each pair of channels was considered as the inverse of the respective weight.
- *Characteristic path length (CPL):* the average shortest path length of the network.
- *Global efficiency (GE):* the average inverse shortest path length of the network.

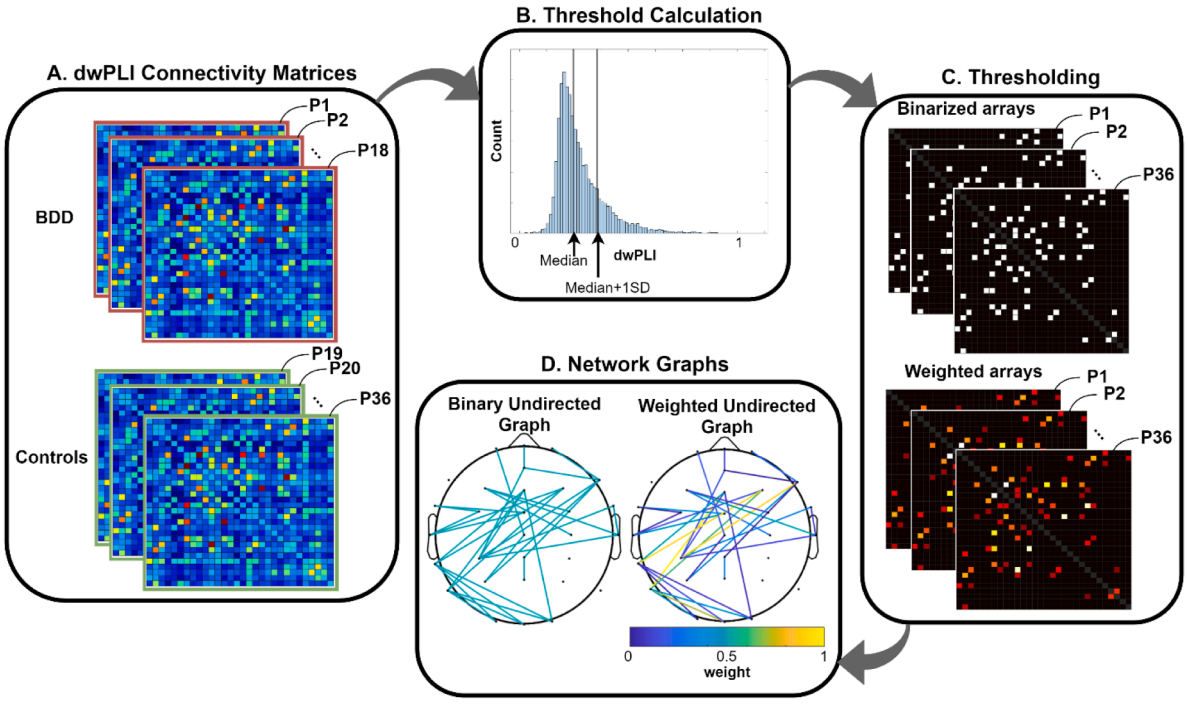

Fig. 2. Processing pipeline for the extraction of network graphs. The procedure converts the all-to-all connectivity matrices at a particular frequency band (panel A) into binary and weighted graph representations (panel D). The functional connectivity measure is the undirected dwPLI between all pairs of channels. The same approach was followed for the directed PSI networks by calculating the threshold (panel B) as the Median + 1SD across the absolute PSI values and ditching the edges with |PSI|<threshold.

2.6.4. Statistical evaluation

Statistical analyses varied between three approaches depending on whether we compared (i) the functional networks (i.e. the edges that survived in dwPLI/PSI between groups), (ii) the global graph-theoretical measures (i.e. Density, Strength, Ccavg, CPL and GE) and (iii) the electrode-specific graph-theoretical measures (i.e. Degree and CC).

(i) **Functional networks comparisons:** To compare the functional connectivity (dwPLI/PSI networks) between CTL and BDD groups, we used a non-parametric cluster permutation approach (Maris and Oostenveld, 2007). This was preferred to eliminate the biases introduced by multiple comparisons and distribution assumptions of parametric tests, since the difference distribution for CTL vs BDD networks is constructed in a data-driven manner using label randomizations combined with a network-based statistic (NBS; Zalesky et al., 2010). Specifically, we conducted 5000 iterations using 5000 random permutations across the subjects' labels ('CTL' and 'BDD'). In each iteration, we first calculated the *t*-values (independent *t*-tests) between groups at each edge. The uncorrected *t*-scores with absolute value higher than 2 were then discarded. Then, the edges that survived were clustered in Strong Connected Components (SCCs; partition into subgraphs with the property of having at least one path between all pairs of nodes) depending on whether they reflect identical effects (separate clusters for positive and negative edges). The sum of *t*-scores within each cluster was considered as the cluster *t*-statistic (Zalesky et al., 2010). Subsequently, the difference distribution curve of the group differences was estimated using the maximum cluster *t*-statistic of each permutation. The *t*-critical values were then calculated to align with the significance level of 0.05 (two-tailed). Clusters formed by the actual labels with cluster *t*-statistic exceeding the *t*-critical values were finally identified following an SCC-wise inference on the difference distribution (Zalesky et al., 2010). Fig. 3 depicts the cluster permutation approach for comparing the functional networks between groups.

(ii) **Global measures:** The global graph-theoretical measures resulted in a single scalar value for each participant and frequency band. To compare those metrics, we used mixed-factor 2×5 ANOVAs with *Group* as a between-subject factor and *Band* as a within-subject factor. Post-hoc comparisons were conducted in case of significant effects using independent *t*-tests. Sphericity violations were adjusted by Greenhouse-Geisser corrections and the two-tailed alpha was set at 0.05.

(iii) **Local measures:** Since the local measures are extracted by each channel, cluster permutation tests were used to correct for multiple comparisons (across 30 channels). We followed the similar approach described in (i), except that: in each iteration, we computed the independent *t*-scores in a channel-by-channel manner and then the clusters were formed according to whether the significant effects were spatially neighbored and had the same sign (positive or negative). This allowed us to identify clusters of neighboring electrodes that showed the same effects on a particular band. The cluster *t*-statistic was also the sum of *t*-scores within each cluster and the *t*-critical values were derived by 5000 random permutations.

2.7. Correlation between EEG and BDD severity

To investigate potential associations between the psychometric (DCQ, YBOCS-BDD scores) and EEG connectivity data (derived by Sections 3.2 and 3.3), separate multiple stepwise linear regression (MSLR) models were conducted. EEG data considered for possible correlations were those that showed significant connectivity differences between groups both in the undirected and directed network analyses. Firstly, we tested whether the EEG connectivity measures could predict BDD symptomatology. This was done by using an MSLR model with the psychometrics as dependent variables and the EEG data as predictors. Each MSLR model contained an intercept, linear terms for each predictor, and all products of pairs (i.e. interactions) of distinct predictors (squared terms were ignored).

3. Results

3.1. Behavioural results

First, we compared behavioural performance between the BDD and the CTL group. Table 1 summarizes the results of the behavioural data comparisons between groups.

3.1.1. Correctness

There was no significant difference in correctness between groups ($t(34) = 0.36$, $p = 0.72$), with the CTL and BDD groups showing 55.0±

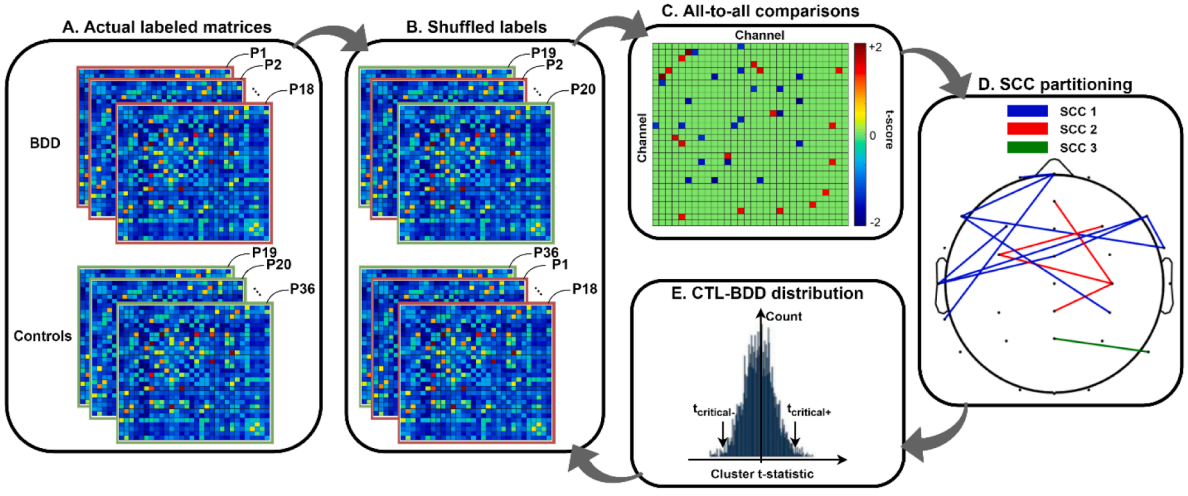

Fig. 3. Cluster permutation testing with network-based statistics. **A.** The starting point of each iteration is the connectivity matrices of all subjects. **B.** Random label assignment (CTL or BDD) to each subject. **C.** Edge-by-edge comparisons between the shuffled groups. **D.** In each one of the 5000 random permutations, the uncorrected t-scores are clustered in strong connected components (SCCs), which are represented with different colours on panel D. **E.** The difference distribution of CTL vs BDD is constructed based on the maximum *t* statistic (where *t* statistic is the sum of *t*-scores of all edges within an SCC). The steps B-E are repeated 5000 times and, finally, the t-critical values correspond to one-sided probabilities of 0.025.

Table 1
Behavioural data comparisons between groups (CTL vs BDD). 'SE' stands for the standard error of the mean. Notation '*' indicates a statistically significant difference.

Measure	Description	CTL *Mean*	*SE*	BDD *Mean*	*SE*	Statistics *t*-value (df = 34)	*p*-value
Correctness	% correct answers	55	12.2	53.6	11.6	0.36	0.72
Confidence	Correct	90.15	2.24	88.72	2.25	0.45	0.66
	Incorrect	90.31	2.43	81.56	2.44	2.54	0.016*
Conf. variance	Across trials	207.48	32.08	304.23	27.65	−2.28	0.028*

12.2% and 53.6± 11.6% correctness, respectively.

3.1.2. Confidence

A 2 (correct, incorrect) x 2 (CTL, BDD) ANOVA on confidence revealed that BDD subjects reported significantly lower confidence when responding incorrectly (81.56± 2.44%) compared to the CTL group (90.31± 2.43%) (*answer* × *group* interaction: $F(1,34) = 6.026$, $p = 0.019$, $\eta_p^2 = 0.151$). However, confidence levels were not significantly different between groups when responding correctly ($p = 0.66$). There was no significant main effect of confidence or group.

3.1.3. Confidence variability

The BDD group also exhibited higher confidence variability across trials (304.23± 27.65) compared to the CTL group (207.48± 32.08), indicating increased variability in the confidence levels ($t(34) = -2.28$, $p = 0.028$).

3.2. Undirected connectivity

3.2.1. dwPLI networks

Cluster permutation testing comparing the dwPLI functional networks between CTL vs BDD revealed a significant subgraph component with inter-connected edges in the theta band ($t_{cluster} = -243.5$, $t_{critical-} = -176.6$, $p = 0.005$). As depicted in Fig. 4A, the significant cluster showed stronger phase synchronization in the BDD compared with the CTL group. The theta cluster showed a widespread distribution of network edges, exhibiting high degree of connectivity in fronto-central electrodes (Fig. 4C). Electrode FCz may serve as the 'hub' of this theta cluster showing a degree of 10. To concretely illustrate the properties of the identified cluster, Fig.4B shows the number of connections shared between seven regions of interest (ROIs). Fronto-central nodes primarily show inter-connections with left-temporal and occipital electrodes. There were no significant clusters in the other frequency bands (all *p*'s>0.05).

It is worth noting that the comparisons presented in this section revealed the sub-network showing significant differences in the phase synchronization between groups. Thus, the identified cluster does not necessarily consist of the 'strong' edges of individuals' networks, instead it is a cluster of edges that measured high statistical differences in dwPLI networks between groups. Complementary to this analysis, we used the single-subject thresholded matrices (i.e. strong edges) to extract the graph theoretical measures, as presented in Section 3.2.2.

Since ERP responses are usually reflected as theta band activity, we also tested whether there were ERP differences between groups. Upon calculating the average across trials (i.e. ERP waves referenced to the −200 to 0 baseline period) for each subject, a cluster permutation test was conducted using 5000 randomizations to estimate the group difference distribution. The cluster permutation test considered the time points 1–500ms after the stimulus onset and all the electrodes except FP1,FP2,FPz (as artifact-sensitive channels). There were no statistically significant spatiotemporal clusters (all *p's*=0.13).

In general, midfrontal theta connectivity has been considered as an indication of the degree of performance monitoring (Luft et al., 2013; Vijver et al., 2011). Thus, stronger midfrontal theta connectivity

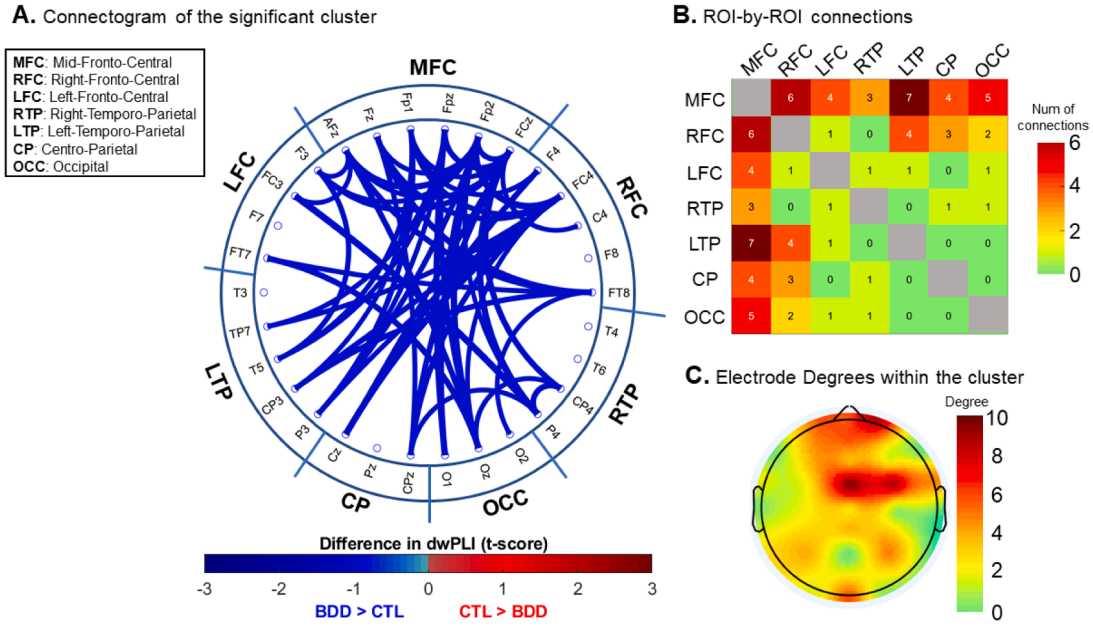

Fig. 4. Undirected network cluster for CTL vs. BDD in theta band. A. Connectogram of the theta band network that showed higher dwPLI in BDD than CTL group. For convenience, the electrodes are also grouped in seven ROIs. Panels B. and C. present the descriptives of the identified significant cluster in the ROI level (B.) and the electrode level (C.). B. Heatmap for the number of connections between each ROI pair of the significant cluster (intra-ROI connections are ignored). C. Scalp topography of the connectivity degree for the identified theta cluster.

suggests that BDD patients show increased performance monitoring activity during decision-making and under uncertainty (McLoughlin et al., 2021).

3.2.2. Undirected graph measures

To further investigate the organizational properties of the undirected networks of CTL vs BDD, the graph theoretical measures were also contrasted. ANOVA on graphs *density* showed a *Band* × *Group* interaction ($F(4, 136) = 3.89$, $p = 0.011$, $\eta_p^2 = 0.103$), but not main effects (p's>0.38). Networks of BDD patients (21.0± 2.3%) showed significantly ($t(34) = -3.8$, $p = 0.001$) higher density than CTL group (11.2 ± 1.0%) in theta band, as shown in Fig. 5A. To localize the effects of density (see Fig. 5C), the cluster permutation testing on *degree* showed a significant negative (BDD>CTL, $t_{cluster} = -17.5$, $t_{critical-} = -8.1$, $p = 0.004$) cluster comprised of fronto-central channels {FP1, FP2, F3, F4, FPz, Afz, Fz}, with BDD showing a fronto-central degree of 6.77± 0.91, whereas that of CTL was 3.21± 0.53. There were no statistically significant outcomes in terms of clustering coefficients, neither in the global *Ccavg* (p's>0.41) nor in the local *CC* (p's>0.072). ANOVA on *CPL* revealed also a significant *Band* × *Group* interaction ($F(4,136) = 3.61$, $p = 0.017$, $\eta_p^2 = 0.096$), with CTL (2.71± 0.12) showing elongated CPL ($t(34) = 3.24$, $p = 0.003$) compared with BDD (2.12± 0.14) only in theta band (see Fig. 5B). As the *GE* is inversely proportional to the CPL, the CTL (0.49± 0.02) showed also reduced ($t(34) = -2.22$, $p = 0.033$) theta GE compared with BDD (0.56± 0.02) group. The effects on CPL/GE suggest that the BDD group recruited more efficient theta connections (and thus higher reachability between pairs of channels) due to the increased densification of their dwPLI networks. Given that the significant measures will be used as predictors in the subsequent correlation analysis (see Section 3.4), and in order to prevent predictor redundancy in the models, we also addressed whether the connectivity measures show dependencies between each other. Fig. 5D illustrates the inter-dependencies of the identified measures, along with the respective correlation coefficients and p-values.

3.3. Directed connectivity

3.3.1. PSI networks

The directed PSI comparisons between CTL vs. BDD revealed a significant cluster of directed edges in alpha band ($t_{cluster} = 161.2$, $t_{critical-} = 141.3$, $p = 0.033$). This cluster showed significantly higher PSI values in CTL than BDD subjects. As depicted in Fig. 6A, the identified cluster showed widespread connections, with dense interconnections from left to midline frontocentral channels. To concretely illustrate the structure of this cluster, Fig. 6B shows the directed connections among seven ROIs. There was a remarkable directed flow indicating that right temporo-parietal (RTP) channels are driven by midline (MFC) and left frontocentral (LFC) regions. In addition, a general lateralized ("left-to-right") flow is observed from the directions of the cluster edges, suggesting that the CTL group shows a more pronounced "left-to-right" lag (i.e. right-hemispheric electrodes were lagged compared to left ones) than the BDD group. Channels F7 and FT7 exhibited the highest number of outward links, mainly driving the MFC electrodes. This left-to-right flow is shown in Fig. 6C, where the maximal outward and inward degrees are observed in left and right electrodes, respectively. There were no significant clusters in the other frequency bands (all p's>0.05).

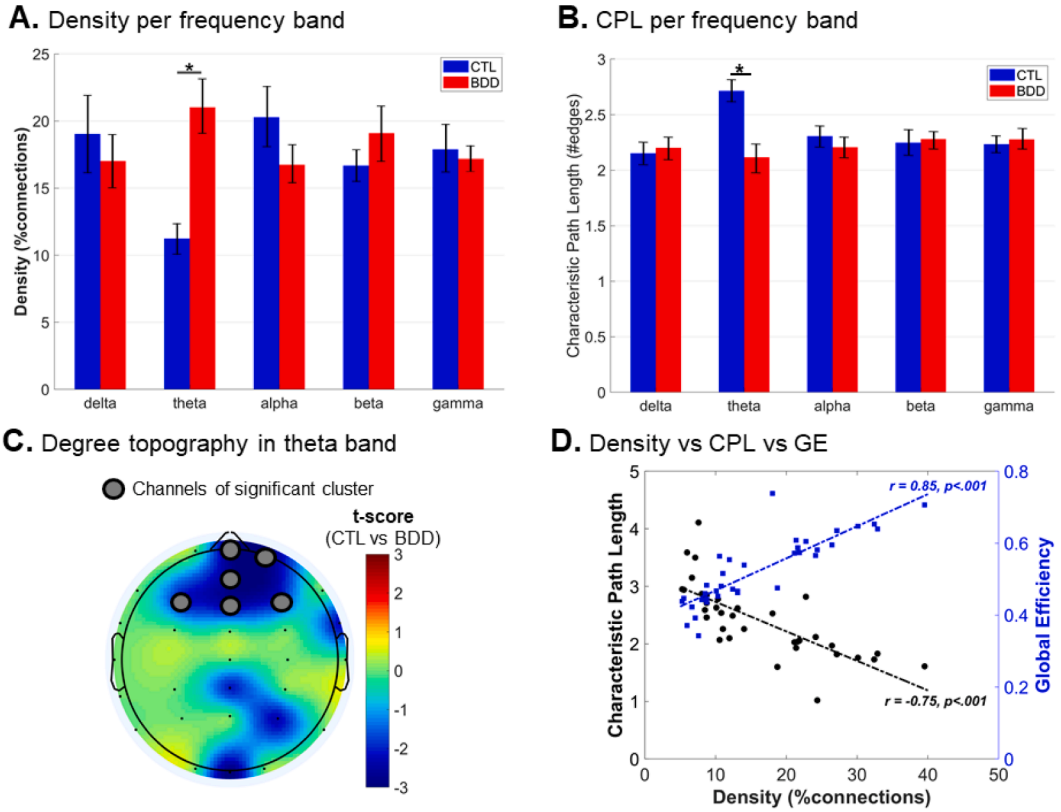

Fig. 5. Undirected graph measures. **A.** Bar graph for *Density* of CTL (blue) and BDD (red) networks in five frequency bands. **B.** Bar graph for *CPL* of CTL (blue) and BDD (red) networks in five frequency bands. Error bars indicate the Mean ± Standard Error. **C.** Scalp topography of t-scores for the *Degree* (CTL vs BDD) comparisons in theta band. Enlarged channels belong to the identified significant cluster. **D.** Scatter plots between *Density* vs *CPL* (left y-axis, black) and *GE* (right y-axis, blue) in theta band. Individual points correspond to single-subject measures. The dashed lines correspond to the best-fitting line curves, accompanied with the respective Pearson's correlation coefficient (r) and the p-value (p). (For interpretation of the references to colour in this figure legend, the reader is referred to the web version of this article.)

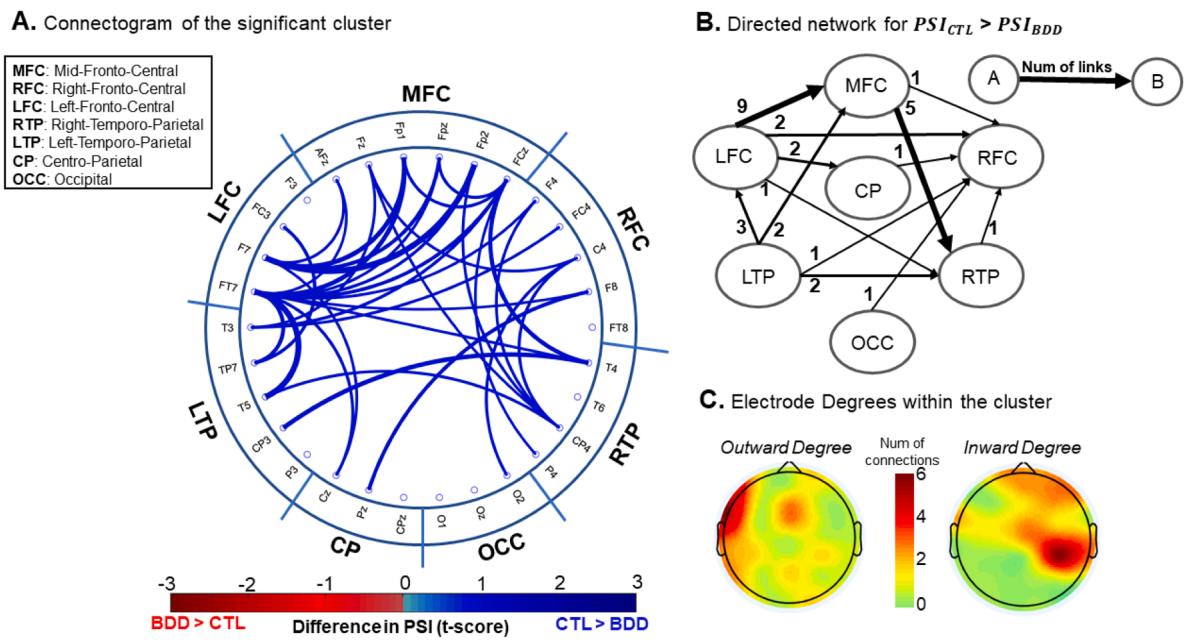

Fig. 6. Directed network cluster for CTL vs BDD in alpha band. **A.** Connectogram of the alpha band network that showed higher PSI in CTL than BDD group. For convenience, the directions are ignored and the electrodes are also grouped in seven ROIs. **B.** Network graph showing the directed connections between ROIs. Above each arrow A->*B*, the number of links interconnecting A and B is also noticed. **C.** Scalp topography of the outward (left) and inward (right) degree for the identified alpha cluster.

Overall, disrupted interhemispheric connectivity in BDD patients has been associated with difficulties integrating detailed information into a coherent whole (J.D. Feusner et al., 2010). Thus, the identified inter-hemispheric difference between the groups could indicate that BDD patients cannot efficiently combine the features of the visual stimuli in order to make a final decision.

3.3.2. *Directed graph measures*

Graph measures extracted from the thresholded PSI matrices were investigated further to give insights about the directed flow of connectivity. Firstly, ANOVA tests yielded no significant effects on the Density (p's>0.086), Strength (p's>0.077) and Degree (p's>0.13). These outcomes suggested that the group differences on PSI (see Section 3.3.1.) are not attributed to alternations in the densification degree of the PSI networks. Instead, since the identified alpha cluster recruited a strong connected component, the group alterations may be attributed to different structural network properties between groups. As depicted in Fig.7A, there was a significant *Band* (p<.001) and *Band* × *Group* interaction ($F(4, 136) = 3.92$, $p = 0.01$, $\eta_p^2 = 0.104$) effects on global clustering coefficient *CCavg*. Planned contrasts at each band showed that the CTL group (0.031± 0.003) presented significantly higher *Ccavg* than the BDD group (0.017± 0.003) only in alpha band ($t(34) = 3.16$, $p = 0.003$). This result implied that the alpha PSI network of the CTL group has stronger clustering properties (i.e. increased number of internal triangles) relative to the BDD group. To localize the scalp areas showing the highest CCs, a cluster permutation on the electrode-specific *CCs* revealed a positive (CTL>BDD, $t_{cluster} = 7.43$, $t_{critical-} = 5.30$, $p = 0.031$) cluster consisting of the right temporo-parietal channels P4, CP4 and T6 (see Fig. 7C for the t-statistic scalp map). Subsequently, the BDD group presented elongated *CPL* (2.51± 0.11), as well as lower *GE*, compared with CTL (2.12± 0.10) group in alpha band (see Fig. 7B). Again, to assess the inter-dependencies between the directed measures, the correlation coefficients were extracted. As shown in Fig. 7D, the *Ccavg* measures were also negatively correlated with the *CPL* (and thus positively correlated with *GE*), since an increased clustering coefficient allows the distances (i.e. shortest paths) between the graph nodes to be reduced.

3.4. *Associations between EEG and psychometrics*

The significant outcomes of the connectivity analyses were further tested for possible correlations with the psychometrics. In summary, two significant connectivity measures were used, namely (i) the undirected degrees in the frontal theta cluster and (ii) the directed clustering coefficient in the right-temporal sites. Other measures (CPL and GE) were excluded from correlation analyses, given their inter-dependencies with the identified EEG measures, as shown in Figs. 5D and 7D, respectively.

The regression model for psychometrics revealed that both the *undirected frontal theta degree* (X_1) and the *directed right temporal clustering coefficient* (X_2) are significant linear predictors of DCQ scores. The model showed a significant overall fit of: $DCQ \sim 11.96 + 0.14 \times X_1 - 1.699 \times X_2; R^2 = 0.39; p < 0.001$. Moreover, YBOCS ratings were well-predicted by only X_2 measures with an overall fit of: $YBOCS \sim 24.15 - 3.34 \times X_2; R^2 = 0.17; p = 0.014$. In Fig. 8, the scatter box-plots of DCQ versus X_1 (Fig. 8A), DCQ versus X_2 (Fig. 8B), YBOCS-BDD versus X_1 (Fig. 8C) and YBOCS-BDD versus X_2 (Fig. 8D) are depicted, along with the respective Pearson's coefficients and p-values.

3.5. *Coexisting spectral differences between groups*

To test for potential underlying spectrum differences between groups, a time-frequency control analysis was conducted (for details see "Supplementary Material"). This approach allowed us to evaluate whether the reported connectivity effects coexist with spectral effects in the same frequency bands considered during connectivity analysis. This analysis revealed significantly higher alpha power in the CTL compared to the BDD group, with the effect being spatially localized in the midline frontal-central-parietal scalp region. There was no significant difference between groups in the theta band (see "Supplementary Material").

4. Discussion

In this study, we investigated the brain connectivity profile of BDD patients relative to healthy controls during decision-making about visual illusions. Results revealed no group differences in susceptibility to visual

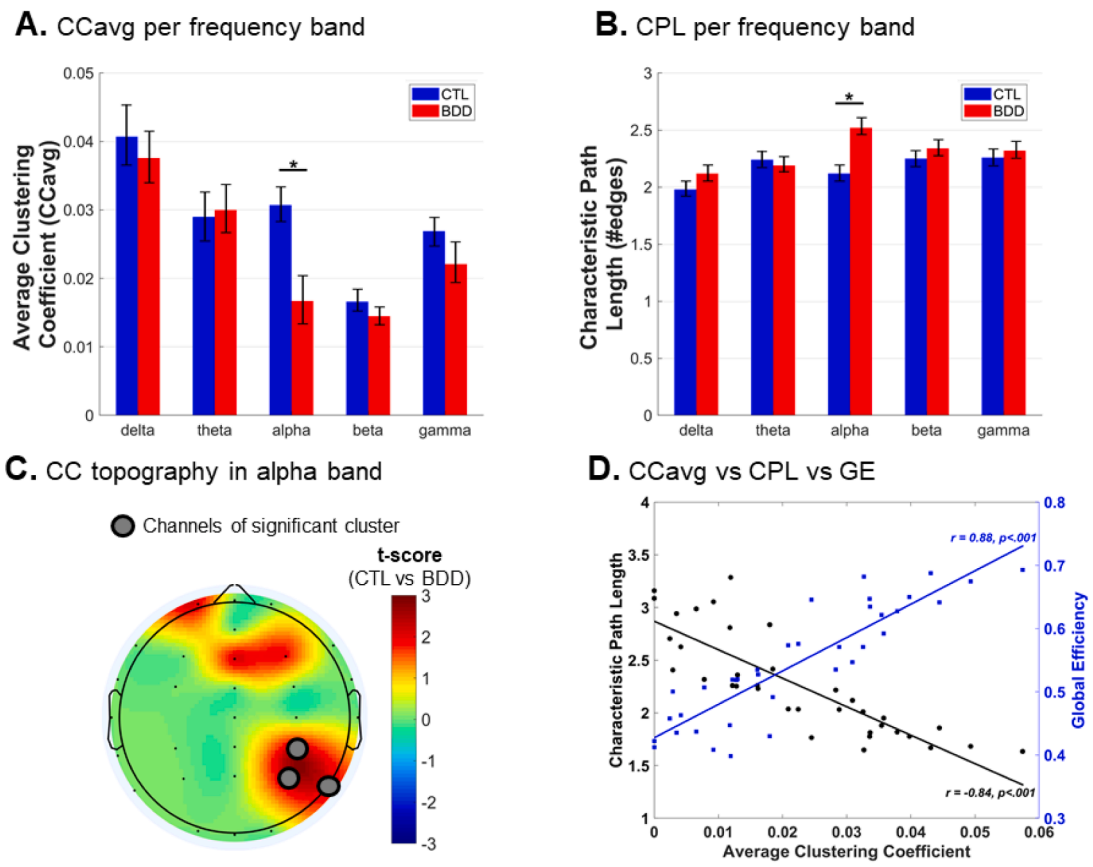

Fig. 7. Directed graph measures. A. Bar graph for Average Clustering Coefficient (Ccavg) of CTL (blue) and BDD (red) networks in five frequency bands. B. Bar graph for CPL of CTL (blue) and BDD (red) networks in five frequency bands. Error bars indicate the Mean ± Standard Error. C. Scalp topography of t-scores for the Clustering Coefficient (CTL vs. BDD) comparisons in alpha band. Enlarged channels belong to the identified significant cluster. D. Scatter plots between Ccavg vs CPL (left y-axis, black) and GE (right y-axis, blue) in alpha band. Individual points correspond to single-subject measures. The lines correspond to the best-fitting line curves, accompanied with the respective Pearson's correlation coefficient I and the p-value (*p*). (For interpretation of the references to colour in this figure legend, the reader is referred to the web version of this article.)

illusions, i.e. both groups perceived the illusory effects to a similar degree. However, the BDD group showed less confidence in their answers compared to the control group, but only when responding incorrectly. Importantly, the BDD patients exhibited higher variability in their confidence levels throughout the session. At the neural level, the BDD group showed greater theta band connectivity when making decisions about visual illusions, indicating widespread synchronization in frontocentral channels. Furthermore, directed connectivity from left to right frontal electrodes in the alpha band was lower in the BDD patients compared to the control group. This effect could be interpreted as less efficient inter-hemispheric communication, and could potentially result from individuals with BDD hyper-focusing on stimulus details. Overall, our findings suggest that performance monitoring processes when making visual judgments might be an important aspect of BDD. This could result in widespread connectivity in midfrontal channels, reflecting constant mental rechecking.

Our first hypothesis was confirmed, as we did not observe a significant difference in susceptibility to the visual illusions in the BDD patients compared to controls. There is evidence to suggest that BDD patients may show enhanced sensitivity in the processing of facial features or details (e.g., Stangier et al., 2008). However, this claim has been disputed considering the lack of differences between BDD patients and controls in the Navon task and other face processing tasks (Monzani et al., 2013). Considering evidence from multiple domains that faces are processed differently from other classes of objects (Bate et al., 2019; McKone and Robbins, 2011), it is possible that BDD patients could show differences in face processing which are not generalized to visual perception. A meta-analysis (Johnson et al., 2018) on the cognitive processes in BDD observed no significant effect of BDD on local visual processing, but mostly higher order effects on selective attention. Their analysis indicated that people with BDD have increased selective attention towards perceived threats (including potential flaws in appearance) which tend to trigger feelings of anxiety and disgust. They also reported findings on abnormalities in memory and suggested that those can account for inaccurate coding and recall of both face and body stimuli. Furthermore, they concluded that these memory issues could trigger maladaptive behaviours, such as constant mirror checking and seeking out cosmetic procedures. Overall, we believe that Johnson et al. (2018) findings might provide evidence that BDD is mostly mediated by higher order cognitive processes instead of lower order visual processing.

As expected, BDD patients reported lower confidence in their visual judgments. In particular, the BDD group was significantly less confident about their answers compared to the CTL group, but that was only the case when they succumbed to the illusory effects. The confidence ratings of the BDD group also fluctuated significantly more compared to controls. These findings are interesting considering that, in our task, participants made judgments from memory, after the visual stimuli were removed from the screen. Not being able to accurately recall the image might have affected participants' confidence levels. It could be that the BDD patients' lower perceptual memory (Johnson et al., 2018) leads them to second-guess their own visual judgments more. These results are in line with previous studies showing that individuals with BDD exhibit high levels of doubt and uncertainty (Hermans et al., 2008; Nedeljkovic

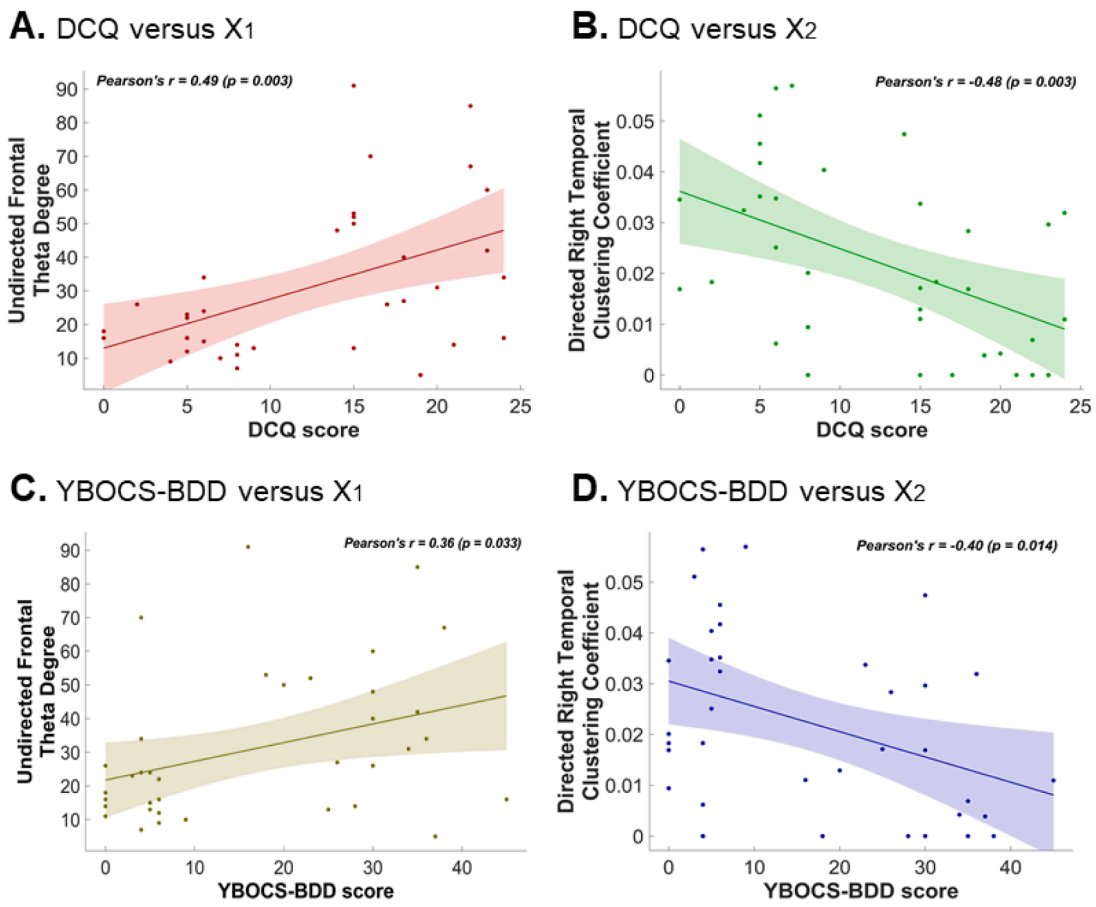

Fig. 8. Relationship between EEG and Psychometrics. A. Scatter plot between DCQ and Undirected Frontal Theta Degree. B. Scatter plot between DCQ and Directed Right Temporal Clustering Coefficient. C. Scatter plot between YBOCS-BDD and Undirected Frontal Theta Degree. D. Scatter plot between YBOCS-BDD and Directed Right Temporal Clustering Coefficient. In the upper part of each panel, the Pearson's correlation coefficient and the respective *p* are notated. Colored-shaded areas correspond to 95% confidence interval.

et al., 2009). Similar to our findings, Tolin et al. (2001) found lower self-reported confidence in OCD patients in a memory recall task, in which participants were repeatedly exposed to threat-related objects. Based on the absence of performance accuracy difference between the OCD and control groups, the authors suggested that confidence differences might reflect increased feelings of doubt in OCD patients, rather than memory deficits, potentially linked to the fact that they often repeat ritualistic behaviours (Tolin et al., 2001).

Notably, the widely observed lack of confidence, lower memory, and excessive monitoring/checking in individuals with BDD could lead to changes in behavior. Widespread differences in cognitive processes such as confidence and memory pose a potential problem, which may call for extra caution when interpreting findings comparing perceptual performance of BDD against controls. For example, Feusner et al. (2011) observed that individuals with BDD showed slower reaction times in a visual perception task, but similar accuracy when compared to the control group, which could reflect the different contribution of these cognitive processes. Thus, when interpreting differences in visual processing between BDD and controls, we need to consider (1) whether the task had a memory component (e.g., matching vs. face memory tasks) and (2) whether the performance was inferred from reaction times, which could be worse if participants feel the need to mentally check their decision, especially in memory-based tasks.

With regards to our brain connectivity findings, there is evidence that connectivity (i.e. interchannel phase synchronization) in midfrontal areas in the theta frequency band is a marker of performance monitoring processes (Luft et al., 2013; Vijver et al., 2011). Therefore, it could be that enhanced theta connectivity in BDD patients might be related to increased cognitive control during excessive activation of the performance monitoring system. In particular, midfrontal theta connectivity might contribute to cognitive control by facilitating information transfer across regions via synchronized phase entrainment (Cavanagh and Frank, 2014). In particular, midfrontal theta activity potentially reflects activation of thalamocortical feedback loops, which have been established as a neural correlate of cognitive control (Cavanagh and Frank, 2014). Furthermore, theta band activity in general plays a role in cross-regional phase synchrony, through the formation of large-scale networks which work together to optimize behavior under uncertainty (McLoughlin et al., 2021; Womelsdorf et al., 2010). Stronger midfrontal theta connectivity could indicate that BDD patients are more intolerant to uncertainty, leading to increased performance monitoring activity during decision-making. It is noteworthy that midfrontal theta connectivity did not correlate with behavioural performance, potentially providing additional evidence that it constitutes a higher order performance monitoring mechanism rather than reflecting actual visual illusion processing.

Furthermore, the BDD group exhibited weaker directed left-to-right hemispheric connectivity in the alpha band compared to the control group. One potential explanation for this could be that individuals with BDD are less capable of contextualizing information, i.e. they are inefficient in combining the elements of the visual scene into a coherent whole (Arienzo et al., 2013). Both BDD and OCD patients have previously demonstrated poor visuospatial construction and memory, which can be attributed to selective recall of details instead of large elements, and could be associated with their clinical features (Deckersbach et al., 2000). This has also been evidenced in neuroimaging studies showing

disrupted interhemispheric connectivity (via the corpus callosum) in BDD patients (Buchanan et al., 2013), potentially reflecting difficulties in integrating detailed information into a coherent whole (Feusner et al., 2010a). Therefore, it could be that, when BDD patients recalled a given visual stimulus in order to make their decision, they evaluated its parts separately, unable to efficiently combine them. On the contrary, the control group might have been more successful in integrating the details into a coherent image, due to better regulation of communication between hemispheres during recall and evaluation of the illusions.

Considering that the control group showed stronger left-to-right and front-to-back directed connectivity, another explanation could be that there is higher top-down modulation in the control group compared to the BDD. Specifically, it could be that controls have increased directed, top-down modulation of the sensory areas while making a decision, potentially representing access to visual information. On the contrary, our findings suggest that BDD patients have increased performance monitoring associated with double checking their responses, rather than accessing the visual memory component itself. Previous neurophysiological studies on bistable and illusory perception have also linked connectivity patterns to percept categories (e.g., Rassi et al., 2022, 2019). In particular, increased prestimulus connectivity from the fusiform face area (FFA) to the primary visual cortex (V1) in lower frequencies predicted face (vs. vase) percepts both in the Rubin face/vase illusion (Rassi et al., 2019), as well as in a face/house binocular rivalry task (Rassi et al., 2022). Previous neuroimaging studies have further shown that the prefrontal cortex performs top-down modulatory control of perceptual inputs (Miller and D'Esposito, 2005; Miller and Cohen, 2001) via interactions between frontal and posterior regions (Bressler et al., 2008; Gregoriou et al., 2009). In line with this, an fMRI study employing a retro-cue paradigm demonstrated higher functional connectivity between frontal and posterior occipital regions which was attributed to top-down modulation (Kuo et al., 2011). Furthermore, it has been suggested that alpha phase synchronization organizes top-down control and access to memory (Klimesch et al., 2010), as observed in studies demonstrating that long-distance alpha phase coherence between the frontal and posterior regions might provide a mechanism underlying top-down modulation of color feature processing (Zanto et al., 2010, 2011). Therefore, our findings corroborate the possibility that BDD is characterized by higher-order disruptions in top-down communication, coupled with inefficient information contextualization during recall. These disruptions are likely attributable to constant performance monitoring and double-checking as opposed to lower-order impairments in visual processing.

Interestingly, we also found a difference in alpha power between groups (see SuppMat.pdf), with the BDD group showing lower alpha activity at the midline fronto-centro-parietal channels during the post-stimulus period. In principle, alpha oscillatory activity is considered vital to attentional processes (Foxe, and Snyder, 2011). Specifically, alpha is suggested to actively inhibit task-irrelevant brain regions (Jensen, and Mazaheri, 2010). The role of alpha is to guide attention by suppressing the impact of distracting inputs, which enhances processing of task-relevant stimuli (Jensen and Mazaheri, 2010). Accordingly, reduced alpha band activity has been related to impairments in the inhibitory mechanisms responsible for eliminating task-irrelevant distractors. In line with this, it has been found that OCD patients show reduced alpha activity during wakeful-resting condition compared to healthy controls (Pogarell et al., 2006). Given that BDD patients have attentional deficits, possibly linked to hyperactivity of the selective attention-related circuits (Bucci et al., 2004), our findings might be explained as a synergy between (i) the reduced inhibition of task-irrelevant stimuli in BDD and (ii) the over-attention of BDD patients during illusory perception.

The simultaneous presence of alpha power and alpha PSI-based connectivity effects is a limitation of this study, especially with respect to interpreting directed alpha connectivity. On the one hand, the observed power and connectivity effects (stronger for the CTL than BDD group) in the alpha band cannot be easily disentangled, since connectivity was computed through a measure which is robust to volume conduction, namely the PSI (Nolte et al., 2008). The connectivity between EEG channels is calculated as the sum of the true connectivity, volume conduction artifacts and noise. Using measures that are blind to volume conduction, only the second term is mitigated towards isolating the true connectivity. In this sense, dwPLI/PSI metrics measure non-instantaneous synchronization which makes the connectivity measures independent of power (Vinck et al., 2011). Furthermore, the fact that we did not find a power effect in the theta band (despite the connectivity effect) may provide some additional evidence that power and connectivity effects are not necessarily coupled in our study. Nevertheless, although the simultaneous power and connectivity effect does not necessarily indicate a volume conduction artifact, a potential carryover effect between power and connectivity during illusory perception needs to be investigated further in future replication studies.

5. Conclusions

In this study, we investigated the susceptibility of BDD patients to visual illusory effects, and their respective brain connectivity patterns while they were making decisions about the corresponding visual stimuli. BDD patients showed an equal degree of susceptibility to illusory effects as controls. However, the BDD group was less confident in their answers when responding incorrectly, and their confidence levels were more variable than controls. We also observed stronger theta synchronization in fronto-central electrodes in BDD patients, which might be associated with excessive activity in their performance monitoring system. Lower alpha connectivity from the left to right hemisphere in BDD patients might indicate issues with inter-hemispheric communication, potentially resulting from less efficient global processing. Connectivity measures of midfrontal theta and inter-hemispheric alpha activity that showed differences between groups were significantly correlated to illness severity in BDD. Overall, these findings shed light on the neurophysiological signature underlying psychopathology in BDD.

Funding information

The study was funded by the Regional Governor of Attica and co-funded by the Athanasios and Marina Matinou Foundation (AMMF) – a non-profit civil company 'AEGEAS'. Dr Caroline Di Bernardi Luft would like to acknowledge the funding from BIAL Foundation (No. 138/18).

CRediT authorship contribution statement

Anastasios E. Giannopoulos: Conceptualization, Methodology, Software, Formal analysis, Writing – original draft, Visualization. **Ioanna Zioga:** Conceptualization, Methodology, Software, Formal analysis, Writing – original draft, Visualization. **Caroline Di Bernardi Luft:** Methodology, Software, Formal analysis, Writing – review & editing, Visualization. **Panos Papageorgiou:** Writing – review & editing. **Georgios N. Papageorgiou:** Writing – review & editing. **Fotini Kapsali:** Resources, Data curation. **Konstantinos Kontoangelos:** Investigation. **Christos N. Capsalis:** Validation, Writing – review & editing, Supervision. **Charalabos Papageorgiou:** Conceptualization, Validation, Investigation, Resources, Supervision, Project administration, Funding acquisition.

Declaration of Competing Interest

The authors declare no conflicts of interest.

Acknowledgments

We would like to thank Dr Alexandros Pantazis and Dr Emmanouil A. Kitsonas for their contribution in the conception and technical implementation on the experimental procedure. We also thank Dr Rachel Bennetts for insightful comments and feedback on the interpretation of our findings. Finally, we would like to warmly thank Dr Rachel Bennetts for proofreading the paper.

Supplementary materials

Supplementary material associated with this article can be found, in the online version, at doi:10.1016/j.psychres.2023.115256.

References

American Psychiatric Association, 2013. Diagnostic and Statistical Manual of Mental Disorders (DSM-5®), 5th ed. American Psychiatric Pub.

Arienzo, D., Leow, A., Brown, J., Zhan, L., GadElkarim, J., Hovav, S., Feusner, J., 2013. Abnormal brain network organization in body dysmorphic disorder. Neuropsychopharmacology 38 (6), 1130–1139.

Bate, S., Bennetts, R., Tree, J., Adams, A., Murray, E., 2019. The domain-specificity of face matching impairments in 40 cases of developmental prosopagnosia. Cognition 192, 104031.

Bennetts, R.J., Gregory, N.J., Tree, J., Luft, C.D.B., Banissy, M.J., Murray, E., Bate, S., 2022. Face specific inversion effects provide evidence for two subtypes of developmental prosopagnosia. Neuropsychologia 174, 108332.

Beucke, J., Sepulcre, J., Buhlmann, U., Kathmann, N., Moody, T., Feusner, J., 2016. Degree connectivity in body dysmorphic disorder and relationships with obsessive and compulsive symptoms. Eur. Neuropsychopharmacol. 26 (10), 1657–1666.

Beucke, J., Sepulcre, J., Talukdar, T., Linnman, C., Zschenderlein, K., Endrass, T., Kathmann, N., 2013. Abnormally high degree connectivity of the orbitofrontal cortex in obsessive-compulsive disorder. JAMA Psychiatry 70 (6), 619–629.

Bora, E., Harrison, B., Fornito, A., Cocchi, L., Pujol, J., Fontenelle, L., Yücel, M., 2011. White matter microstructure in patients with obsessive–compulsive disorder. J. Psychiatry & Neurosci. JPN 36 (1), 42.

Bressler, S.L., Tang, W., Sylvester, C.M., Shulman, G.L., Corbetta, M., 2008. Top-down control of human visual cortex by frontal and parietal cortex in anticipatory visual spatial attention. J. Neurosci. 28 (40), 10056–10061. https://doi.org/10.1523/JNEUROSCI.1776-08.2008.

Bruno, N., 2005. Unifying sequential effects in perceptual grouping. Trends Cogn. Sci. (Regul. Ed.) 9 (1), 1–3.

Buchanan, B., Rossell, S., Maller, J., Toh, W., Brennan, S., Castle, D., 2013. Brain connectivity in body dysmorphic disorder compared with controls: a diffusion tensor imaging study. Psychol. Med. 43 (12), 2513–2521.

Bucci, P., Mucci, A., Volpe, U., Merlotti, E., Galderisi, S., Maj, M., 2004. Executive hypercontrol in obsessive–compulsive disorder: electrophysiological and neuropsychological indices. Clin. Neurophysiol. 115 (6), 1340–1348.

Buhlmann, U., McNally, R., Etcoff, N., Tuschen-Caffier, B., Wilhelm, S., 2004. Emotion recognition deficits in body dysmorphic disorder. J. Psychiatr. Res. 201–206.

Buhlmann, U., McNally, R.J., Wilhelm, S., Florin, I., 2002. Selective processing of emotional information in body dysmorphic disorder. J. Anxiety Disord. 16 (3), 289–298.

Cavanagh, J.F., Zambrano-Vazquez, L., Allen, J.J., 2012. Theta lingua franca: a common mid-frontal substrate for action monitoring processes. Psychophysiology 49 (2), 220–238. https://doi.org/10.1111/J.1469-8986.2011.01293.X.

Cavanagh, J., Frank, M., 2014. Frontal theta as a mechanism for cognitive control. Trends Cogn. Sci. (Regul. Ed.) 18 (8), 414–421.

Chaumon, M., Bishop, D.V., Busch, N.A., 2015. A practical guide to the selection of independent components of the electroencephalogram for artifact correction. J. Neurosci. Methods 250, 47–63.

Chennu, S., O'Connor, S., Adapa, R., Menon, D.K., Bekinschtein, T.A., 2016. Brain connectivity dissociates responsiveness from drug exposure during propofol-induced transitions of consciousness. PLoS Comput. Biol. 12 (1), e1004669 https://doi.org/10.1371/JOURNAL.PCBI.1004669.

Deckersbach, T., Savage, C.R., Phillips, K.A., Wilhelm, S., Buhlmann, U., Rauch, S.L., Jenike, M.A., 2000. Characteristics of memory dysfunction in body dysmorphic disorder. J. Int. Neuropsychol. Soc. 6 (6), 673–681.

Delorme, A., Makeig, S., 2004. EEGLAB: an open source toolbox for analysis of single-trial EEG dynamics including independent component analysis. J. Neurosci. Methods 134 (1), 9–21.

Eagleman, D., 2001. Visual illusions and neurobiology. Nat. Rev. Neurosci. 2 (12), 920–926.

Feusner, J.D., Moller, H., Altstein, L., Sugar, C., Bookheimer, S., Yoon, J., Hembacher, E., 2010a. Inverted face processing in body dysmorphic disorder. J. Psychiatr. Res. 44 (15), 1088–1094.

Feusner, J.D., Moody, T., Hembacher, E., Townsend, J., McKinley, M., Moller, H., Bookheimer, S., 2010b. Abnormalities of visual processing and frontostriatal systems in body dysmorphic disorder. Arch. Gen. Psychiatry 67 (2), 197–205.

Feusner, J., Hembacher, E., Moller, H., Moody, T., 2011. Abnormalities of object visual processing in body dysmorphic disorder. Psychol. Med. 41 (11), 2385–2397.

Foxe, J.J., Snyder, A.C., 2011. The role of alpha-band brain oscillations as a sensory suppression mechanism during selective attention. Front. Psychol. 2, 154.

Garibotto, V., Scifo, P., Gorini, A., Alonso, C., Brambati, S., Bellodi, L., Perani, D., 2010. Disorganization of anatomical connectivity in obsessive compulsive disorder: a multi-parameter diffusion tensor imaging study in a subpopulation of patients. Neurobiol. Dis. 37 (2), 468–476.

Giannopoulos, A., Zioga, I., Kontoangelos, K., Papageorgiou, P., Kapsali, F., Capsalis, C. N., Papageorgiou, C., 2022. Deciding on optical illusions: reduced alpha power in body dysmorphic disorder. Brain Sci. 12, 293. https://doi.org/10.3390/brainsci12020293.

Giannopoulos, A., Zioga, I., Papageorgiou, P., Kapsali, F., Spantideas, S., Kapsalis, N., Papageorgiou, C., 2021. Early auditory-evoked potentials in body dysmorphic disorder: an ERP/sLORETA study. Psychiatry Res. 299, 113865.

Grace, S., Labuschagne, I., Kaplan, R., Rossell, S., 2017. The neurobiology of body dysmorphic disorder: a systematic review and theoretical model. Neurosci. Biobehav. Rev. 83, 83–96.

Gregoriou, G.G., Gotts, S.J., Zhou, H., Desimone, R., 2009. High-frequency, long-range coupling between prefrontal and visual cortex during attention. Science 324 (5931), 1207–1210. https://doi.org/10.1126/SCIENCE.1171402.

Gregory, R., 1997. Visual illusions classified. Trends Cogn. Sci. (Regul. Ed.) 1 (5), 190–194.

Hermans, D., Engelen, U., Grouwels, L., Joos, E., Lemmens, J., Pieters, G., 2008. Cognitive confidence in obsessive-compulsive disorder: distrusting perception, attention and memory. Behav. Res. Ther. 46 (1), 98–113.

Jensen, O., Mazaheri, A., 2010. Shaping functional architecture by oscillatory alpha activity: gating by inhibition. Front. Hum. Neurosci. 4, 186.

Johnson, S., Williamson, P., Wade, T., 2018. A systematic review and meta-analysis of cognitive processing deficits associated with body dysmorphic disorder. Behav. Res. Ther. 107, 83–94.

Kapsali, F., Nikolaou, P., Papageorgiou, C., 2019. Yale-brown obsessive compulsive scale modified for body dysmorphic disorder (BDD-YBOCS): greek translation, validation and psychometric properties. EC Psychol. Psychiatry 8, 884–894. https://doi.org/10.3389/fnins.2018.00654.

Kapsali, F., Zioga, I., Papageorgiou, P., Smyrnis, N., Chrousos, G.P., Papageorgiou, C., 2020. Event-related EEG oscillations in body dysmorphic disorder. Eur. J. Clin. Invest. 50 (3), e13208. https://doi.org/10.1111/eci.13208.

King, D.J., Hodgekins, J., Chouinard, P.A., Chouinard, V.A., Sperandio, I., 2017. A review of abnormalities in the perception of visual illusions in schizophrenia. Psychon. Bull. Rev. 24 (3), 734–751. https://doi.org/10.3758/S13423-016-1168-5.

Klimesch, W., Freunberger, R., Sauseng, P., 2010. Oscillatory mechanisms of process binding in memory. Neurosci. Biobehav. Rev. 34 (7), 1002–1014.

Kuo, B., Yeh, Y., Chen, A., D'Esposito, M, 2011. Functional connectivity during top-down modulation of visual short-term memory representations. Neuropsychologia 49 (6), 1589–1596.

Luft, C.D.B., Nolte, G., Bhattacharya, J., 2013. High-learners present larger mid-frontal theta power and connectivity in response to incorrect performance feedback. J. Neurosci. 33 (5), 2029–2038.

Maris, E., Oostenveld, R., 2007. Nonparametric statistical testing of EEG-and MEG-data. J. Neurosci. Methods 164 (1), 177–190.

Mataix-Cols, D., Wooderson, S., Lawrence, N., Brammer, M., Speckens, A., Phillips, M., 2004. Distinct neural correlates of washing, checking, and hoarding symptomdimensions in obsessive-compulsive disorder. Arch. Gen. Psychiatry 61 (6), 564–576.

McKone, E., & Robbins, R. (2011). Are faces special. In *Oxford Handbook of Face Perception* (pp. 149–176).

McLoughlin, G., Gyurkovics, M., Palmer, J., Makeig, S., 2021. Midfrontal theta activity in psychiatric illness: an index of cognitive vulnerabilities across disorders. Biol. Psychiatry.

Miller, B., D'Esposito, M, 2005. Searching for "the top" in top-down control. Neuron 48 (4), 535–538.

Miller, E., Cohen, J., 2001. An integrative theory of prefrontal cortex function. Annu. Rev. Neurosci. Retrieved from http://www.annualreviews.org/doi/abs/10.1146/annurev.neuro.24.1.167.

Mognon, A., Jovicich, J., Bruzzone, L., Buiatti, M., 2011. ADJUST: an automatic EEG artifact detector based on the joint use of spatial and temporal features. Psychophysiology 48 (2), 229–240. https://doi.org/10.1111/j.1469-8986.2010.01061.x.

Monzani, B., Krebs, G., Anson, M., Veale, D., Mataix-Cols, D., 2013. Holistic versus detailed visual processing in body dysmorphic disorder: testing the inversion, composite and global precedence effects. Psychiatry Res. 210 (3), 994–999.

Murray, M.M., Herrmann, C.S., 2013. Illusory contours: a window onto the neurophysiology of constructing perception. Trends Cogn. Sci. (Regul. Ed.) 17 (9), 471–481.

Nedeljkovic, M., Moulding, R., Kyrios, M., Doron, G., 2009. The relationship of cognitive confidence to OCD symptoms. J. Anxiety Disord. 23 (4), 463–468.

Nolan, H., Whelan, R., Reilly, R.B., 2010. FASTER: fully automated statistical thresholding for EEG artifact rejection. J. Neurosci. Methods 192 (1), 152–162.

Nolte, G., Ziehe, A., Nikulin, V.V., Schlögl, A., Krämer, N., Brismar, T., Müller, K.R., 2008. Robustly estimating the flow direction of information in complex physical systems. Phys. Rev. Lett. (23), 100. https://doi.org/10.1103/PhysRevLett.100.234101.

Oostenveld, R., Fries, P., Maris, E., Schoffelen, J., 2011. FieldTrip: open source software for advanced analysis of MEG, EEG, and invasive electrophysiological data. Comput. Intell. Neurosci. 2011, 1.

Oosthuizen, P., Lambert, T., Castle, D.J., 1998. Dysmorphic concern: prevalence and associations with clinical variables. Aust. N. Z. J. Psychiatry 32 (1), 129–132. https://doi.org/10.1046/j.1440-1614.1998.00377.x.

Papageorgiou, C., Stachtea, X., Papageorgiou, P., Alexandridis, A.T., Makris, G., Chrousos, G., Kosteletos, G., 2020. Gender-dependent variations in optical illusions: evidence from N400 waveforms physiological measurement gender-dependent variations in optical illusions: evidence from N400 waveforms. Physiol. Meas. 41 (9), 095006 https://doi.org/10.1088/1361-6579/abb2eb.

Perera, M.P.N., Bailey, N.W., Herring, S.E., Fitzgerald, P.B., 2019. Electrophysiology of obsessive compulsive disorder: a systematic review of the electroencephalographic literature. J. Anxiety Disord. 62, 1–14.

Phillips, K.A., Hollander, E., Rasmussen, S.A., Aronowitz, B.R., 1997. A severity rating scale for body dysmorphic disorder: development, reliability, and validity of a modified version of the Yale-Brown Obsessive Compulsive Scale. Psychopharmacol. Bull. 33 (1), 17.

Pogarell, O., Juckel, G., Mavrogiorgou, P., Mulert, C., Folkerts, M., Hauke, W., Hegerl, U., 2006. Symptom-specific EEG power correlations in patients with obsessive–compulsive disorder. Int. J. Psychophysiol. 62 (1), 87–92.

Rassi, E., Wutz, A., Müller-Voggel, N., Weisz, N., 2019. Prestimulus feedback connectivity biases the content of visual experiences. Proc. Natl Acad. Sci. 116 (32), 16056–16061.

Rassi, E., Wutz, A., Peatfield, N., Weisz, N., 2022. Efficient prestimulus network integration of fusiform face area biases face perception during binocular rivalry. J. Cogn. Neurosci. 34 (6), 1001–1014.

Stam, C., Nolte, G., Daffertshofer, A., 2007. Phase lag index: assessment of functional connectivity from multi channel EEG and MEG with diminished bias from common sources. Hum. Brain Mapp. 28 (11), 1178–1193. https://doi.org/10.1002/hbm.20346.

Stangier, U., Adam-Schwebe, S., Müller, T., Wolter, M., 2008. Discrimination of facial appearance stimuli in body dysmorphic disorder. J. Abnorm. Psychol. 117 (2), 435.

Sterzer, P., Rees, G., 2008. A neural basis for percept stabilization in binocular rivalry. J. Cogn. Neurosci. 20 (3), 389–399. https://doi.org/10.1162/jocn.2008.20039.

Toh, W.L., Castle, D.J., Rossell, S.L., 2015. Examining neurocognition in body dysmorphic disorder using the Repeatable Battery for the Assessment of Neuropsychological Status (RBANS): A. Psychiatry Res. 228 (3), 318–324.

Toh, W.L., Castle, D.J., Rossell, S.L., 2017. Attentional biases in body dysmorphic disorder (bdd): eye-tracking using the emotional Stroop task. Compr. Psychiatry 74, 151–161.

Tolin, D.F., Abramowitz, J.S., Brigidi, B.D., Amir, N., Street, G.P., Foa, E.B., 2001. Memory and memory confidence in obsessive–compulsive disorder. Behav. Res. Ther. 39 (8), 913–927.

Vijver, I.Van de, Ridderinkhof, K., Cohen, M, 2011. Frontal oscillatory dynamics predict feedback learning and action adjustment. J. Cogn. Neurosci. 23 (12), 4106–4121.

Vinck, M., Oostenveld, R., Van Wingerden, M., Battaglia, F., Pennartz, C.M.A., 2011. An improved index of phase-synchronization for electrophysiological data in the presence of volume-conduction, noise and sample-size bias. Neuroimage 55 (4), 1548–1565. https://doi.org/10.1016/j.neuroimage.2011.01.055.

Winkler, I., Haufe, S., Tangermann, M., 2011. Automatic classification of artifactual ICA-components for artifact removal in EEG signals. Behav. Brain Funct. 7 (1), 30. https://doi.org/10.1186/1744-9081-7-30.

Womelsdorf, T., Johnston, K., Vinck, M., Everling, S., 2010. Theta-activity in anterior cingulate cortex predicts task rules and their adjustments following errors. Proc. Natl. Acad. Sci. 107 (11), 5248–5253.

Yaryura-Tobias, J., Neziroglu, F., Chang, R., Lee, S., Pinto, A., Donohue, L., 2002. Computerized perceptual analysis of patients with body dysmorphic disorder: a pilot study. CNS Spectr. 7 (6), 444–446. https://doi.org/10.1017/S1092852900017958.

Zalesky, A., Fornito, A., Bullmore, E., 2010. Network-based statistic: identifying differences in brain networks. Neuroimage 53 (4), 1197–1207.

Zanto, T., Rubens, M., Bollinger, J., Gazzaley, A., 2010. Top-down modulation of visual feature processing: the role of the inferior frontal junction. Neuroimage 53 (2), 736–745.

Zanto, T., Rubens, M., Thangavel, A., Gazzaley, A., 2011. Causal role of the prefrontal cortex in top-down modulation of visual processing and working memory. Nat. Neurosci. 14 (5), 656–661.